

1
2
3 1
4
5

6 2 **Title (English):** Comparison of supervised and unsupervised automatic classification
7
8 3 methods for sediment types mapping using multibeam echosounder and grab sampling
9

10
11 4
12
13

14 5 **Title (Italian):**
15
16

17
18 6
19

20
21 7 **Authors:** Ibon Galparsoro ^{*1}, Xabier Agrafojo¹, Marc Roche² & Koen Degrendele²
22
23

24 8 **Affiliations:**
25
26

27 9 ¹ AZTI-Tecnalia; Marine Research Division; Herrera Kaia, Portualdea z/g; 20110
28
29 10 Pasaia (Spain); *corresponding author's e-mail: igalparsoro@azti.es. Tel: +34
30
31 11 667174450.
32
33

34
35 12 ² FPS Economy, S.M.E.s, Self-employed and Energy. Quality and Security. Continental
36
37 13 Shelf; Bd du Roi Albert II, 16 - 1000 (Belgium).
38
39

40
41 14
42

43 15 **Abstract**
44
45

46 16 Multibeam echosounder (MBES) systems are effective seabed mapping tools due to
47
48 17 their simultaneous bathymetry and backscatter data acquisition. The acoustic response
49
50 18 of the seafloor can be used to infer some of the physical characteristics of the sediment.
51
52 19 However, further development and formalization of the methodology is still required.
53
54 20 This investigation evaluates the ability to perform an automatic classification of
55
56
57
58
59
60

1
2
3 21 sediment types with MBES data by using both unsupervised and supervised (with *in situ*
4
5 22 sediment samples) digital image classification algorithms.
6
7

8
9 23 The case-study focussed on an area near the Basque coast, northern Spain (SE Bay of
10
11 24 Biscay). The seafloor morphological aspects were calculated from a digital elevation
12
13 25 model derived from datasets acquired with a SeaBat 7125 MBES, while the backscatter
14
15 26 information was recorded with an EM3002D MBES. The parameters considered for the
16
17 27 automatic classification were seabed rugosity, slope, backscatter amplitude mean level
18
19 28 and backscatter variance. A total of 58 sediment grab samples were used for supervised
20
21 29 automatic classification training and validation.
22
23

24
25 30 Results showed that supervised classification obtained higher precision than the
26
27 31 unsupervised classification (76.9% and 30.8%, respectively) and higher reliability (0.7
28
29 32 and 0.2, respectively). According to these results, the unsupervised classification could
30
31 33 be considered useful as a first estimate of the spatial distribution of seafloor types, but
32
33 34 should only be used in studies where *in situ* samples are not available. In contrast,
34
35 35 supervised classification demonstrated its ability to discriminate more sedimentary
36
37 36 facies than the unsupervised classification and was especially effective in areas where
38
39 37 the seabed displayed heterogeneous features and multiple sediment types. The result of
40
41 38 this investigation confirms the potential of MBES and automatic classification
42
43 39 algorithms for the production of classified maps of sedimentary types, with sufficient
44
45 40 reliability for different applications, including management purposes.
46
47
48
49

50 41

51
52
53 42 **Keywords:** Multibeam echosounder, acoustic backscatter, automatic classification,
54
55 43 sediment characteristics.
56
57
58
59
60

1
2
3 44
4
5
6 45
7
8
9 46
10
11
12
13
14
15
16
17
18
19
20
21
22
23
24
25
26
27
28
29
30
31
32
33
34
35
36
37
38
39
40
41
42
43
44
45
46
47
48
49
50
51
52
53
54
55
56
57
58
59
60

Riassunto and parole chiave

For Review Only

1. Introduction

During the last decades, the intensity and diversification of the exploitation of living and non-living resources in seas and oceans has increased significantly. For the management of these limited natural resources, the availability of thematic seabed maps is of high strategic interest. This need for detailed information regarding depth, seafloor features and seafloor types distribution, motivated the development of a wide range of techniques, with an emphasis on remote hydro-acoustic techniques. Nevertheless, the morphological distribution patterns and sedimentologic features of the seafloor is usually very complex. It is particularly difficult to achieve high reliability in the mapping of continuous variables (e.g. grain size distribution), and the conclusions derived solely based on *in situ* samples (i.e. grab and cores) can result in a misunderstanding of the spatial scales of the distribution of the characteristics of the seabed (Ellingsen, 2002). For this reason, the research on hydro-acoustic techniques focuses on the improvement of the accuracy and resolution of the obtained data, in order to achieve maximum detail and subsequently unravel the complexity of the seabed. In particular, the development of multibeam echosounder (MBES) systems allowed the collection simultaneously of detailed depth and reflectivity data with a comprehensive acoustic coverage (Hughes-Clarke *et alii*, 1996; Kenny, 2003). Therefore, MBES is an excellent seabed mapping tool (Brown & Blondel, 2009a).

Conventionally, the identification and interpretation of seafloor types and of morphological features using hydro-acoustic data, are accomplished with the input of expert human judgement. To facilitate the analysis of data from large areas, several methods for automatic classification of bottom types have been developed (Rooper & Zimmermann, 2007; Rzhhanov *et alii*, 2012; Simons & Snellen, 2009; van Walree *et alii*,

1
2
3 71 2005). These techniques were designed to allow a faster and more objective processing.
4
5 72 Several automatic classification algorithms have been applied to characterize the
6
7 73 substrates based on seafloor bathymetry and backscatter data (Brown *et alii*, 2011; Che
8
9 74 Hasan *et alii*, 2012; Fonseca & Mayer, 2007; Ierodionou *et alii*, 2011; Lamarche *et*
10
11 75 *alii*, 2011; Stephens & Diesing, 2014). Moreover, these methods have also
12
13 76 demonstrated great potential to predict benthic habitats and communities (Brown &
14
15 77 Blondel, 2009b; Cutter Jr *et alii*, 2003; Herzfeld & Higginson, 1996; Lucieer & Lucieer,
16
17 78 2009; Lüdtke *et alii*, 2012). Although automatic methods have demonstrated high
18
19 79 potential to segment the acoustic reflectivity in similar regions, they have not been fully
20
21 80 accepted by the scientific community as a tool to produce systematic and reliable maps
22
23 81 (Brown *et alii*, 2011). The numerous sources of error and uncertainty when using
24
25 82 automatic classification algorithms affect the final classification accuracy. Among the
26
27 83 most important sources of uncertainty, Ierodionou *et alii*. (2011) highlighted: the
28
29 84 proper classification method employed; the quality of MBES records; the quality of the
30
31 85 data used in defining classes of bottom types (or habitats); the adequacy of seafloor
32
33 86 variables to define classes (e.g. slope, rugosity, reflectivity); the ability to integrate
34
35 87 observations and hydro-acoustic data; and the complexity in setting the boundaries for
36
37 88 defining classes to categorise the seafloor.
38
39
40
41
42
43

44 89 The objective set out in this research was to compare automatic methods of supervised
45
46 90 and unsupervised classification, based on MBES records and sediment samples from an
47
48 91 experimental area, and to establish which of both, unsupervised or supervised
49
50 92 classification algorithms, provides the most reliable map of sediment type; in other
51
52 93 words, analyse whether the incorporation of information from sediment samples in the
53
54 94 process of automatic classification improves the accuracy and reliability of the resulting
55
56 95 sediment type distribution map.
57
58
59
60

1
2
3 96 **2. Material and methods**

4
5 97 **2.1. Regional setting**

6
7
8 98 The study area was located in the SE Bay of Biscay (northern Spain) and covers an area
9
10 99 of 0.32 km² (Figure 1). The seabed in this sector shows a high morphological diversity.
11
12 100 The interaction of tectonic activity, basement topography and sea-level changes,
13
14 101 together with processes of sediment supply and prevailing climatic conditions
15
16 102 (Galparsoro *et alii*, 2010) have a critical influence on the configuration of the
17
18 103 continental shelf seascapes and the distribution of seafloor material. In particular, strong
19
20 104 NW swell waves dominate and are the most common sea state within the study area
21
22 105 (González *et alii*, 2004). Under extreme offshore wave conditions, significant wave
23
24 106 heights can exceed 5 m (several times a year) and, occasionally, 10 m (with return
25
26 107 periods of 20 years) (Liria *et alii*, 2009). Thus, sediment dynamics are produced by
27
28 108 wave dominated processes, which in turn, are responsible of the transport and shaping
29
30 109 of the sandbanks.
31
32
33
34
35

36 110 In particular, the study area is characterised by a shallow rocky belt extending from the
37
38 111 coastline up to 35-40 m depth and the presence of a paleo-channel. Sedimentary seabed
39
40 112 extends from 35-40 m up to 80 m depth and it is characterised by the diversity of
41
42 113 sediment types; from coarse sands up to fine mud (Figure 1). Several bedforms, such as
43
44 114 sorted bedforms and mega-ripple fields, reflect the sediment dynamics produced by the
45
46 115 action of currents and waves on the seafloor in this sector (Galparsoro *et alii*, 2010).
47
48 116 The morphology of the seabed indicates that the influence of wave action reaches down
49
50 117 to 50 m depth. In the southeast, the presence of marks of dredged material disposal was
51
52 118 also identified.
53
54
55

56
57 119
58
59
60

120 2.2. Data sets

121 2.2.1. Bathymetry and backscatter information

122 Two surveys were conducted with two different MBES. Surveys were carried out in
123 June 2011 within two weeks time in order to guarantee the same seafloor conditions.
124 The morphological aspects were derived from a digital elevation model produced from
125 SeaBat 7125 MBES records. This MBES operates at 400 kHz, producing 256 beams in
126 a 128° angle swath and using up to 50 swaths per second. The beam width is 0.5° along-
127 track and 1° across-track, producing very small footprints (for more details see
128 Galparsoro, et alii., (2009)). The MBES was coupled with an Agp132 (TRIMBLE)
129 global position system, receiving differential corrections. An OCTANS III (IXSEA)
130 gyrocompass and motion sensor was utilised, to compensate for the movement of the
131 vessel. Furthermore, a portable SVP 15 (RESON) was used, to measure sound velocity
132 profiles throughout the entire water column every two hours during the survey. The
133 software package PDS2000 was used to integrate the MBES data, with the information
134 from all the auxiliary sensors during the surveys—data acquisition and synchronization.
135 This software was used in real-time, as well as in the post-processing of the integrated
136 data. Tidal correction was applied using records from a tide gauge located at Bilbao
137 harbour and 1m resolution seafloor Digital Elevation Model (DEM) was produced in
138 projected coordinate UTM, Zone 30 N (WGS84).

139 The backscatter data was recorded with a Kongsberg Simrad EM 3002D MBES. The
140 system uses two angle mounted sonar heads, producing a total of 508 individual beams
141 with a maximum swath width of 200°. The opening angle of each beam is 1.5° and the
142 pulse length is 150µs. The sound frequency was set to 300 kHz. The MBES was
143 interfaced with a Thales Aquarius GPS, receiving differential corrections. The data were

1
2
3 144 corrected in real-time, for roll, pitch and heave, using a Seatex MRU5 motion sensor
4
5 145 and, for heading, using an Anschütz Standard 20 gyrocompas. Two sound velocity
6
7 146 profiles were measured with a "Sea-Bird" SBE19 (Seacat) STD system before and after
8
9 147 the survey. A fixed Valeport mini SVS probe installed next to the starboard antenna was
10
11 148 used to measure continuously the sound velocity values at the transducer. The
12
13 149 acquisition software SIS from Kongsberg was used to integrate the MBES data, with the
14
15 150 data from the auxiliary sensors. The data were post-processed with Kongsberg Neptune
16
17 151 for the bathymetry. Tidal correction was applied using the nearest tide gauge. DEM and
18
19 152 backscatter mosaic were computed at 1 m resolution in projected coordinate UTM,
20
21 153 Zone 30 N (WGS84). Backscatter records were processed using the algorithm
22
23 154 Geocoder, implemented in the Fledermaus software (Interactive Visualization Systems)
24
25 155 (Fonseca & Mayer, 2007). Default processing parameters were chosen: adjusting
26
27 156 (Tx/Rx power gain correction, beam pattern correction, no beam angle cut-off, use of
28
29 157 the logged calibrated backscatter range) and filtering (flat Angle Varying Gain (AVG)
30
31 158 correction with a window of 30).
32
33
34
35
36

37 2.2.2. Sediment samples

38
39
40 160 Sedimentologic characteristics were derived from 58 surficial grab samples
41
42 161 corresponding to the period from 1994 up to 2011 (Galparsoro *et alii*, 2010) (see Figure
43
44 162 1 and Table 1). Sediment analysis was carried out using dry sieving method and Laser
45
46 163 Diffraction Particle Size Analyser (LDPSA). In order to homogenise both data sets, a
47
48 164 transformation was applied to the results obtained with LDPSA, to refer all data to the
49
50 165 results obtained by dry sieving (Rodríguez & Uriarte, 2009).
51
52
53
54
55
56
57
58
59
60

168 **2.2.3. Underwater images**

169 Fourteen seafloor image recording locations were selected based on morphological
170 features of the seabed derived from MBES data records and sedimentologic information
171 derived from grab samples (see Figure 1). Images were recorded with a Kongsberg
172 Simrad OE14-112 (PAL; Horizontal Resolution 460 TV Lines) installed in a still frame
173 and georeferenced with a DGPS. These were used for the subsequent visual interpretation
174 of the classification of sedimentary types obtained by automatic classification.

175 **2.3. Seafloor classification**

176 **2.3.1. Sediment classes definition**

177 The definition of the sediment classes was based on sediment grain size (Blott & Pye
178 (2001), Udden (1914) and Wentworth (1922)). The defined classes were: (1) Coarse and
179 very coarse sand (CS and VCS) (-1-to 1phi; 500µm-2mm); (2) Medium sands (MS) (1-
180 2phi, 250-500µm); (3) Fine sand (FS) (2-3phi, 125-250µm); and (4) Very fine sand
181 (VFS) (3-4phi; 63 - 125µm). Coarse and very coarse sands classes were grouped into a
182 one single class due to the limited number of samples for these classes. Thus, the total
183 number of samples for each sedimentary class were: CS and VCS = 13; MS = 7; FS =
184 28; and VFS = 10.

185 On the other hand, the seabed morphological and backscatter variables (derived from
186 MBES) considered for the automatic classification were : (1) depth; (2) backscatter
187 amplitude; (3) slope; (4) texture (derived from the analysis of variance of backscatter);
188 and (5) seabed rugosity. Rugosity was calculated as a measure of terrain complexity,
189 defined as the ratio of surface area to planar area. It was calculated using ArcGIS
190 extension Benthic Terrain Modeler (BTM), Version 1.0 (Wright *et alii*, 2005). Those
191 information layers were standardized to a pixel size of 5 meters and the variables were

1
2
3 192 re-scaled to values between 0 and 100. All outliers were removed by conditional
4
5 193 expressions to avoid their participation in the classification process.
6
7

8 194 **2.3.2. Automatic classifications**

9
10
11 195 A non-supervised classification applying the Isodata method (Ball & Hall, 1965) was
12
13 196 conducted using (ArcGIS 9.3). This is an iterative automatic classification algorithm
14
15 197 based on the minimum spectral distance function (Iterative Self-Organizing Data
16
17 198 Analysis Technique). This classification method does not require sediment samples, but
18
19 199 is based on the definition of spectral classes present in the image. Classification of
20
21 200 bottom types is based on the grouping of areas with similar characteristics (Chuvieco &
22
23 201 Congalton, 1988). The maximum number of iterations for the process was set at 15 and
24
25 202 a convergence threshold of 0.95 was established. This threshold defines the maximum
26
27 203 percentage of pixels that are kept together in the same class and does not vary between
28
29 204 iterations.
30
31
32
33

34 205 Secondly, Maximum Likelihood was used as the digital supervised classification
35
36 206 algorithm (Chuvieco & Congalton, 1988) implemented in ArcGIS. This method
37
38 207 requires some prior knowledge of the study area. For this research, reference sediment
39
40 208 types (or classes of seabed) defined by the characteristics of grain size of the sediment
41
42 209 samples, were used as observed data. Before the automatic classification, 80% of all
43
44 210 sediment samples were reserved for the training and classification process (i.e. 46
45
46 211 samples) and the remaining 20% were reserved for validation (i.e. 12 samples); this
47
48 212 division was conducted randomly. For each class of seabed, the statistical signature was
49
50 213 calculated. This signature describes the seabed morphological characteristics and
51
52 214 acoustic response of each class. The statistical signatures were used to apply the
53
54 215 classification on the entire study area. Finally, the classified image obtained with the
55
56
57
58
59
60

1
2
3 216 maximum likelihood algorithm was rendered applying a majority filter (in ArcGIS 9.3
4
5 217 software) to replace outlying cells based on the majority of their eight contiguous
6
7 218 neighbouring cells.
8
9

10 219 An accuracy assessment from each classification technique was established with the
11
12 220 calculation of the producer accuracy (PA) and user accuracy (UA); for the total
13
14 221 classification, and for each of the classes (Stehman, 1997). The values of producer and
15
16 222 user accuracy were calculated as a percentage. In terms of overall accuracy, the average
17
18 223 accuracy of the producer (the average of all the points of the producer) and the average
19
20 224 accuracy of the user (the average of all the points of the user) were used. Furthermore,
21
22 225 the validity of the overall classification and for each of the sedimentary types, was
23
24 226 expressed with the Kappa statistic (k) (Stehman, 1997). The possible values for k range
25
26 227 between 0 and 1, with the values closer to 1 reflecting the greater confidence in the
27
28 228 classification.
29
30
31
32
33

34 229

35 36 37 230 **3. Results**

38
39
40 231 For each sediment type class considered in this study, the morphological and acoustic
41
42 232 response extracted from the information layer used in the analysis is given in Table 2.
43
44 233 Our results show that the backscatter amplitude values increased as grain size defining
45
46 234 the sediment type increase, except for FS, which showed the lower value. In terms of
47
48 235 slope, CS-VCS was collected on the steepest seafloor and the FS, the flattest. VFS and
49
50 236 MS showed similar slope values. CS-VCS, MS and VFS showed the lower texture
51
52 237 values; meanwhile the FS showed the highest. Finally, no differences were found on the
53
54 238 rugosity of the seafloor.
55
56
57
58
59
60

1
2
3 239 The first run of the unsupervised classification, executed considering all information
4
5 240 layers, resulted in a total classification accuracy of 15.38% and a validity (k) value of
6
7 241 0.16 (Figure 2). The resulting map did not reflect the spatial distribution of the
8
9 242 characteristics of the seabed observed on the backscatter records (Figure 1), especially
10
11 243 for the sorted bedform area where the coarser sediments were located. The bathymetry
12
13 244 probably biased the classification because depth showed a higher percentage of the
14
15 245 variance than the rest of the layers, and as a consequence impeded the input from other
16
17 246 information. For this reason, the depth information was removed for subsequent
18
19 247 analysis on unsupervised and supervised classifications. By doing that, the validation
20
21 248 results obtained showed a significant improvement, with a total classification accuracy
22
23 249 of 30.77% and 76.92% for unsupervised and supervised classifications, respectively
24
25 250 (Table 3). Results obtained for each sediment class indicate that unsupervised
26
27 251 classification was not able to classify VCS-CS and MS sediment classes, and most of
28
29 252 the pixels were classified as being FS and VFS, which was incorrect. In contrast,
30
31 253 supervised classification performed better for all sediment classes. For three of the
32
33 254 sediment classes (i.e. VCS-CS, MS and VFS), all the ground-truthing samples were
34
35 255 classified correctly. The classification performed worse when classifying CS-VCS
36
37 256 pixels. Similar pattern was observed for the validity of the classification. Total validity
38
39 257 values (k) resulted in 0.19 and 0.66, for unsupervised and supervised classifications,
40
41 258 respectively (Table 4). For all sediment classes, supervised classification obtained better
42
43 259 results, and only for FS, kappa value was similar for both classifications.
44
45
46
47
48
49

50 260 The sediment classes distribution maps (Figure 3) and areas (Table 5), derived from the
51
52 261 unsupervised and supervised automatic classification methods, show a similar sediment
53
54 262 classes distribution pattern and areas. Main difference was that supervised classification
55
56 263 assigned higher areas for VCS-CS and FS; and lower areas for MS and VFS, than
57
58
59
60

1
2
3 264 unsupervised classification. A sandy patch surrounded by fine sand was identified by
4
5 265 the supervised classification while the unsupervised classification was not able to
6
7 266 discriminate it (Figure 3). Thus, the supervised classification discriminated more facies
8
9 267 in areas with more irregular morphology, and therefore, the capacity of identification of
10
11 268 higher diversity of sediments deposits.

12
13
14 269 The results of both classifications were corroborated by the images of the seafloor
15
16 270 obtained by underwater video (Figure 4). Differences in the content of biogenic material
17
18 271 (i.e. composition of shells in different parts of the study area) in the surface of the
19
20 272 sediment could be observed, which in turn, have determined the mean grain size of
21
22 273 sediment samples, the acoustic response and the final classification of the map. In areas
23
24 274 of FS and MS bioturbation marks could also be observed; meanwhile, in areas of VFS,
25
26 275 which is distributed up to 50-55m depth, ripple marks produced by wave action are
27
28 276 identifiable.

29
30
31
32
33 277

34 35 36 37 278 **4. Discussion**

38
39
40 279 The ongoing trend toward high resolution MBES has great potential for significant
41
42 280 advances in mapping and characterization of bottom types to better improve our
43
44 281 understanding about seafloor ecosystems (e.g. Brown *et alii.*, (2011)). The present
45
46 282 research has shown that the information obtained by MBES is especially useful in the
47
48 283 process of classification of bottom types (Bellec *et alii.*, 2009; Brown *et alii.*, 2011; Che
49
50 284 Hasan *et alii.*, 2012; Rzhhanov *et alii.*, 2012). In general, our results are consistent with
51
52 285 those studies, which concluded that the low reflectivity normally corresponds to the
53
54 286 "soft" seabed (silt and fine sand) and high reflectivity with the "hard" sediments (gravel,
55
56 287 stones or rock), while the sands and shells have average reflectivity values.

1
2
3 288 The first unsupervised classification (Figure 2) resulted in a very low accuracy and
4
5 289 reliability of the sediment type distribution. The results indicated that the bathymetry
6
7 290 produced interference during the process of automatic classification, due to the higher
8
9 291 weight of the bathymetry layer in the overall variance that biased the result. The
10
11 292 classification did not consider the input of the other characteristics of the seabed (i.e.
12
13 293 backscatter, slope) and resulted in a simple representation of depth ranges. While it is
14
15 294 generally accepted that grain size decreases and mud content increases with increasing
16
17 295 depth, this assumption may only be valid at large scale and depth ranges. On a smaller
18
19 296 spatial scale or in places with complex hydrodynamic processes, such as this case study,
20
21 297 this pattern of distribution of sediment may not be valid (see Table 2). The resulting
22
23 298 map of sediment type distribution was incompatible with structures that were previously
24
25 299 identified from MBES interpretation and expert judgement. For this reason, the digital
26
27 300 elevation model was omitted in subsequent classification processes.
28
29
30
31

32
33 301 The accuracy of the supervised digital classification (Maximum Likelihood algorithm)
34
35 302 and reliability were both significantly better. The reliability value was the maximum for
36
37 303 all the sediment types except for fine sand (Table 4) which lowered total value of kappa.
38
39 304 Fine sand was the sediment type that presented the larger standard deviation for
40
41 305 reflectivity and other parameters used for classification (Table 2). A discrepancy
42
43 306 between the real distribution of sediment types and their representation in the samples,
44
45 307 or an incorrect definition of the classes of sediment type could explain this pattern.
46
47
48

49 308 Another observation was the "noise" in the resulting map obtained from the supervised
50
51 309 classification (Figure 3b). This noise is identifiable as parallel stripes and it is the result
52
53 310 of errors (artefacts) caused by insufficient compensation of the vessel accelerations
54
55 311 during acquisition of bathymetric data. Therefore, it is an artefact drawn by the lower
56
57
58
59
60

1
2
3 312 quality of the original data used for the extraction of morphological characteristics of
4
5 313 the seabed. This phenomenon, however, is less evident in the result of the unsupervised
6
7 314 classification (Figure 3a).
8
9

10 315 In terms of the relation between sediment type and reflectivity, it was observed that the
11
12 316 fine sand, contrary to what might be expected, had a lower value of reflectivity than the
13
14 317 very fine sand. This could in turn affect the final result of the automatic classification
15
16
17 318 and thus, the reliability of the map. The content of mud, could be the reason of the
18
19 319 acoustic response of the very fine sand. The possible effect of infauna communities on
20
21 320 the acoustic response of the sediment should also be considered. In this regard, it is
22
23 321 recommended for future research to use other sediment physical characteristics such as
24
25 322 porosity, compaction or lithological composition and characterization of benthic
26
27 323 communities.
28
29

30
31 324 It could be assumed that automatic classification methods may not have the same
32
33 325 reliability as the classification derived from human interpretation and expert judgment,
34
35 326 but it could be stated that the sediment type distribution maps obtained from automatic
36
37 327 classification methods, show an acceptable accuracy and reliability for many research
38
39 328 and management purposes. The main advantage of these automatic algorithms is that
40
41 329 they allow processing of a much higher volumes of information in less time and in an
42
43 330 objective way. Moreover, the resulting maps could be validated and their accuracy and
44
45 331 reliability could be calculated. The resulting maps could contribute towards a better
46
47 332 understanding of the complexity and irregularity of the seabed, particularly in
48
49 333 sedimentary substrates, which is of great importance in the interpretation of sedimentary
50
51 334 processes and distribution of communities and benthic habitats.
52
53
54
55

56
57 335
58
59
60

336 5. Conclusions

337 Seafloor thematic maps (i.e. seafloor types, sediment distribution maps) are essential
338 source of information to assist in the knowledge of the spatial distribution of the living
339 and non-living resources. Moreover, they are an important source of information to
340 understand ecosystem processes that could be used for estimating the environmental
341 impact that could be produced by human activities and the adoption of new spatially-
342 based management measures. The results obtained in this research support the idea that
343 the image-based classification of the seabed (i.e. morphological characteristics and
344 acoustic response) shows considerable promise for the use of MBES data for the
345 production of thematic maps. Moreover, periodical surveys of coastal areas could also
346 be useful to determine the changes and evolution of the seabed; especially in areas
347 hosting intense human activities that can cause physical changes as dredging processes,
348 dredged material disposal, underwater infrastructure or fishing activity.

349 This research has demonstrated the ability to produce reliable sediment type distribution
350 maps based on multibeam echo sounding data, sediment samples and automatic
351 classification algorithms. The results show that the incorporation of information from
352 field samples in the classification process (supervised classification) significantly
353 improved the accuracy and reliability of the resulting seabed sediment classification.
354 We conclude that unsupervised classification is valid for an initial approximation of the
355 spatial distribution of bottom types or studies in which there is no *in situ* sedimentologic
356 information available, but the results should be considered with caution because of the
357 high dependence on the choice of variables.

358 The extraction of information on the characteristics of the seabed from geophysical
359 parameters has great potential but needs further development of techniques to process

1
2
3 360 data and further progress in the understanding of the relation between the acoustic
4
5 361 response of seafloor and its physical and biological characteristics.
6
7

8 362
9

10 11 363 **Acknowledgements** 12 13

14 364 This manuscript is a result of the projects MeshAtlantic (Atlantic Area Transnational
15
16 365 Cooperation Programme 2007-2013 of the European Regional Development Fund)
17
18 366 (www.meshatlantic.eu) and DEVOTES (DEvelopment Of innovative Tools for
19
20 367 understanding marine biodiversity and assessing good Environmental Status) funded by
21
22 368 the European Union under the 7th Framework Program 'The Ocean of Tomorrow'
23
24 369 Theme (grant agreement no. 308392) (www.devotes-project.eu). Authors would like to
25
26 370 thank to Dr. Guillem Chust and Mireia Valle for their valuable comments in the first
27
28 371 version of the manuscript. We would also like to thank Caroline Lavoie for the
29
30 372 exhaustive review and improvement of the manuscript. This paper is contribution
31
32 373 number XXX from AZTI-Tecnalia (Marine Research Division).
33
34
35
36
37
38
39
40

41 375 **References** 42 43

- 44 376 Ball, G. H., Hall, D. J. (1965) - *Isodata, a novel method of data analysis and pattern*
45 377 *classification*. Editor: Stanford Research Institute, California
46 378 Bellec, V. K., Dolan, M. F. J., Bøe, R., Thorsnes, T., Rise, L., Buhl-Mortensen, L., Buhl-
47 379 Mortensen, P. (2009) - *Sediment distribution and seabed processes in the Troms II area*
48 380 *- offshore North Norway*. Norwegian Journal of Geology, **89**, 29-40.
49 381 Blott, S. J., Pye, K. (2001) - *GRADISTAT: a grain size distribution and statistics package for*
50 382 *the analysis of unconsolidated sediments*. Earth Surface Processes and Landforms, **26**,
51 383 1237-1248.
52 384 Brown, C. J., Blondel, P. (2009a) - *The application of underwater acoustics to seabed habitat*
53 385 *mapping*. Applied Acoustics, **70**, 1241.
54 386 Brown, C. J., Blondel, P. (2009b) - *Developments in the application of multibeam sonar*
55 387 *backscatter for seafloor habitat mapping*. Applied Acoustics, **70**, 1242-1247.
56
57
58
59
60

- 1
2
3 388 Brown, C. J., Todd, B. J., Kostylev, V. E., Pickrill, R. A. (2011) - *Image-based classification of*
4 389 *multibeam sonar backscatter data for objective surficial sediment mapping of Georges*
5 390 *Bank, Canada*. Continental Shelf Research, **31**, S110-S119.
- 6 391 Cutter Jr, G. R., Rzhanov, Y., Mayer, L. A. (2003) - *Automated segmentation of seafloor*
7 392 *bathymetry from multibeam echosounder data using local Fourier histogram texture*
8 393 *features*. Journal of Experimental Marine Biology and Ecology, **285–286**, 355-370.
- 9 394 Che Hasan, R., Ierodiaconou, D., Laurenson, L. (2012) - *Combining angular response*
10 395 *classification and backscatter imagery segmentation for benthic biological habitat*
11 396 *mapping*. Estuarine, Coastal and Shelf Science, **97**, 1-9.
- 12 397 Chuvieco, E., Congalton, R. G. (1988) - *Using cluster analysis to improve the selection of*
13 398 *training statistics in classifying remotely sensed data*. Photogrammetric Engineering &
14 399 *Remote Sensing*, **54**, 1275-1281.
- 15 400 Ellingsen, K. E. (2002) - *Soft-sediment benthic biodiversity on the continental shelf in relation*
16 401 *to environmental variability*. Marine Ecology Progress Series, **232**, 15-27.
- 17 402 Fonseca, L., Mayer, L. (2007) - *Remote estimation of surficial seafloor properties through the*
18 403 *application Angular Range Analysis to multibeam sonar data*. Marine Geophysical
19 404 *Researches*, **28**, 119-126.
- 20 405 Galparsoro, I., Borja, Á., Bald, J., Liria, P., Chust, G. (2009) - *Predicting suitable habitat for*
21 406 *the European lobster (Homarus gammarus), on the Basque continental shelf (Bay of*
22 407 *Biscay), using Ecological-Niche Factor Analysis*. Ecological Modelling, **220**, 556-567.
- 23 408 Galparsoro, I., Borja, Á., Legorburu, I., Hernández, C., Chust, G., Liria, P., Uriarte, A. (2010) -
24 409 *Morphological characteristics of the Basque continental shelf (Bay of Biscay, northern*
25 410 *Spain); their implications for Integrated Coastal Zone Management*. Geomorphology,
26 411 **118**, 314-329.
- 27 412 González, M., Uriarte, A., Fontán, A., Mader, J., Gyssels, P. (2004) - Marine dynamics. Pages
28 413 133-157 in *Oceanography and Marine Environment of the Basque Country* Elsevier
29 414 *Oceanography Series*.
- 30 415 Herzfeld, U. C., Higginson, C. A. (1996) - *Automated geostatistical seafloor classification—*
31 416 *Principles, parameters, feature vectors, and discrimination criteria*. Computers &
32 417 *Geosciences*, **22**, 35-52.
- 33 418 Hughes-Clarke, J. E., Mayer, L. A., Wells, D. E. (1996) - *Shallow-Water Imagin Multibeam*
34 419 *Sonars: A New Tool for Investigating Seafloor Processes in the Coastal Zone and on*
35 420 *the Continental Shelf*. Marine Geophysical Researches, **18**, 607-629.
- 36 421 Ierodiaconou, D., Monk, J., Rattray, A., Laurenson, L., Versace, V. L. (2011) - *Comparison of*
37 422 *automated classification techniques for predicting benthic biological communities using*
38 423 *hydroacoustics and video observations*. Continental Shelf Research, **31**, S28-S38.
- 39 424 Kenny, A. (2003) - *An overview of seabed-mapping technologies in the context of marine*
40 425 *habitat classification*. ICES Journal of Marine Science, **60**, 411-418.
- 41 426 Lamarche, G., Lurton, X., Verdier, A.-L., Augustin, J.-M. (2011) - *Quantitative*
42 427 *characterisation of seafloor substrate and bedforms using advanced processing of*
43 428 *multibeam backscatter--Application to Cook Strait, New Zealand*. Continental Shelf
44 429 *Research*, **31**, S93-S109.
- 45 430 Liria, P., Garel, E., Uriarte, A. (2009) - *The effects of dredging operations on the*
46 431 *hydrodynamics of an ebb tidal delta: Oka Estuary, northern Spain*. Continental Shelf
47 432 *Research*, **29**, 1983-1994.
- 48 433 Lucieer, V., Lucieer, A. (2009) - *Fuzzy clustering for seafloor classification*. Marine Geology,
49 434 **264**, 230-241.
- 50 435 Lüdtke, A., Jerosch, K., Herzog, O., Schlüter, M. (2012) - *Development of a machine learning*
51 436 *technique for automatic analysis of seafloor image data: Case example, Pogonophora*
52 437 *coverage at mud volcanoes*. Computers & Geosciences, **39**, 120-128.
- 53 438 Rodríguez, J. G., Uriarte, A. (2009) - *Laser Diffraction and Dry-Sieving Grain Size Analyses*
54 439 *Undertaken on Fine- and Medium-Grained Sandy Marine Sediments: A Note*. Journal of
55 440 *Coastal Research*, **25**, 257-264.
- 56
57
58
59
60

- 1
2
3 441 Rooper, C. N., Zimmermann, M. (2007) - *A bottom-up methodology for integrating underwater*
4 442 *video and acoustic mapping for seafloor substrate classification*. Continental Shelf
5 443 *Research*, **27**, 947-957.
6 444 Rzhanov, Y., Fonseca, L., Mayer, L. (2012) - *Construction of seafloor thematic maps from*
7 445 *multibeam acoustic backscatter angular response data*. Computers & Geosciences, **41**,
8 446 181-187.
9 447 Simons, D. G., Snellen, M. (2009) - *A Bayesian approach to seafloor classification using multi-*
10 448 *beam echo-sounder backscatter data*. Applied Acoustics, **70**, 1258-1268.
11 449 Stehman, S. V. (1997) - *Selecting and interpreting measures of thematic classification*
12 450 *accuracy*. Remote Sensing of the Environment, **62**, 77-89.
13 451 Stephens, D., Diesing, M. (2014) - *A Comparison of Supervised Classification Methods for the*
14 452 *Prediction of Substrate Type Using Multibeam Acoustic and Legacy Grain-Size Data*.
15 453 PLoS ONE, **9**, e93950.
16 454 Udden, J. A. (1914) - *Mechanical composition of clastic sediments*. Bulletin Geological Society
17 455 of America, **25**, 655-744.
18 456 van Walree, P. A., Tęgowski, J., Laban, C., Simons, D. G. (2005) - *Acoustic seafloor*
19 457 *discrimination with echo shape parameters: A comparison with the ground truth*.
20 458 Continental Shelf Research, **25**, 2273-2293.
21 459 Wentworth, C. K. (1922) - *A scale of grade and class terms for clastic sediments*. Journal of
22 460 Geology, **30**, 377-392.
23 461 Wright, D. J., Lundblad, E. R., Larkin, E. M., Rinehart, R. W. (2005) - *Benthic Terrain*
24 462 *Modeller Toolbar*. Oregon State University Davey Jones Locker Seafloor
25 463 *Mapping/Marine GIS Lab*. http://dusk.geo.orst.edu/esri04/p1433_ron.html.
26 464
27 465
28
29
30
31
32
33
34
35
36
37
38
39
40
41
42
43
44
45
46
47
48
49
50
51
52
53
54
55
56
57
58
59
60

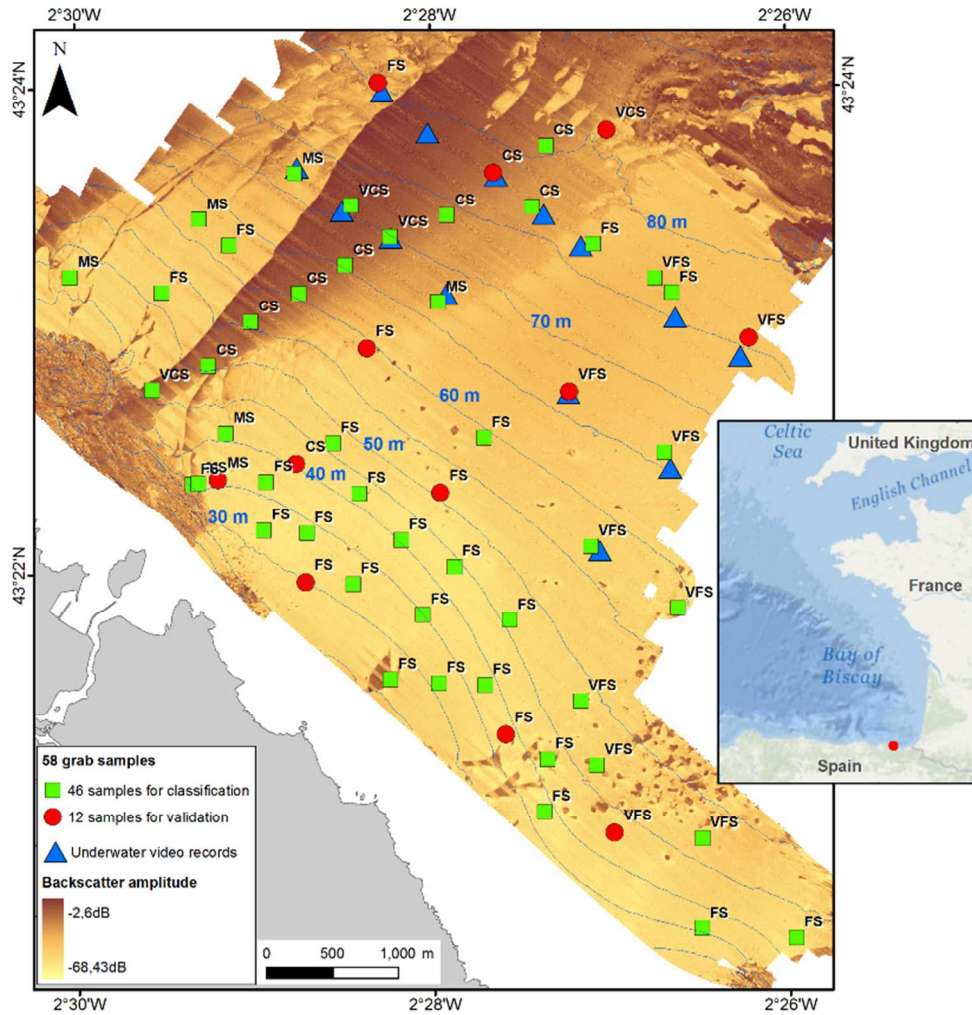


Figure 1. Study area location within the SE Bay of Biscay. Multibeam echosounder derived acoustic backscatter and the spatial distribution of sediment grab samples, classified into the ones used for the automatic classification process and the validation of the resulting classification, are shown (VCS: very coarse sand; CS: coarse sands; MS: medium sand; FS: fine sand; and VFS: very fine sand). Locations in which underwater videos were recorded are also represented.
71x73mm (300 x 300 DPI)

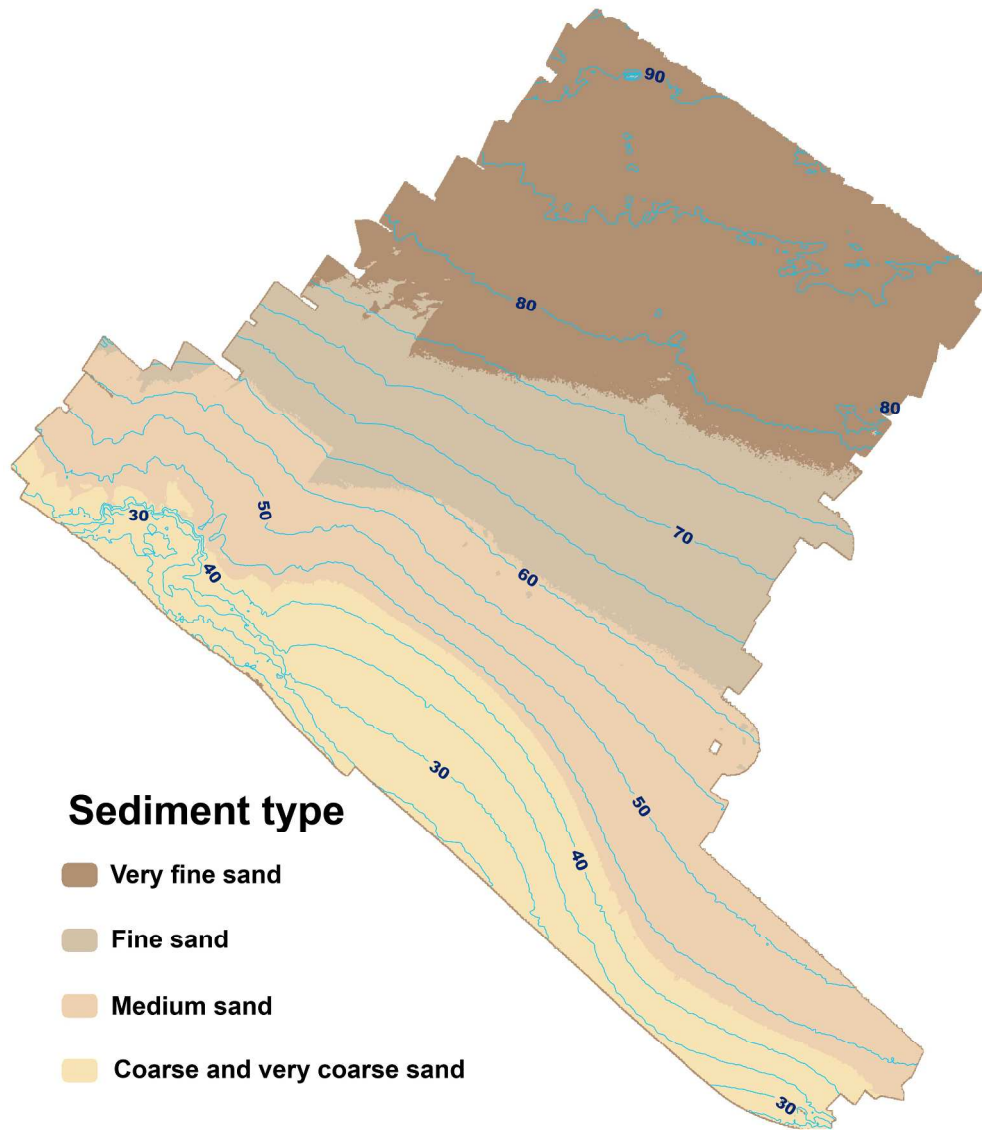


Figure 2. Sediment type distribution map resulting from the application of an unsupervised classification with bathymetry, backscatter amplitude, slope, texture and rugosity information layers. Total classification accuracy: 15.38% and a validity (k) value of 0.16. Interpretation of the result suggests a bathymetry biased classification.
414x476mm (220 x 220 DPI)

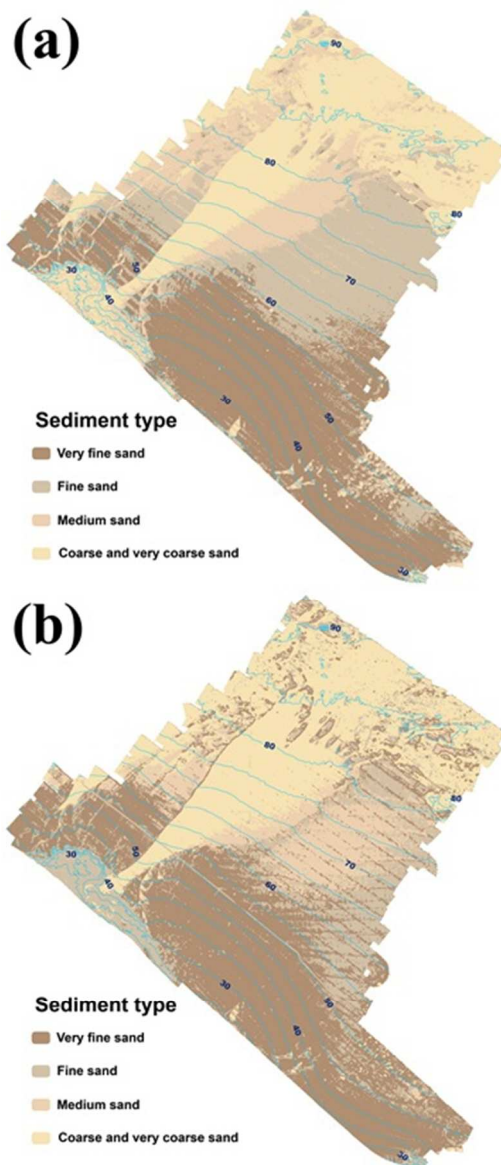


Figure 3. Sediment type distribution map resulting from the application of an unsupervised classification (a) and supervised classification (b) with backscatter amplitude, slope, texture and rugosity information layers. 30x71mm (300 x 300 DPI)

1
2
3
4
5
6
7
8
9
10
11
12
13
14
15
16
17
18
19
20
21
22
23
24
25
26
27
28
29
30
31
32
33
34
35
36
37
38
39
40
41
42
43
44
45
46
47
48
49
50
51
52
53
54
55
56
57
58
59
60

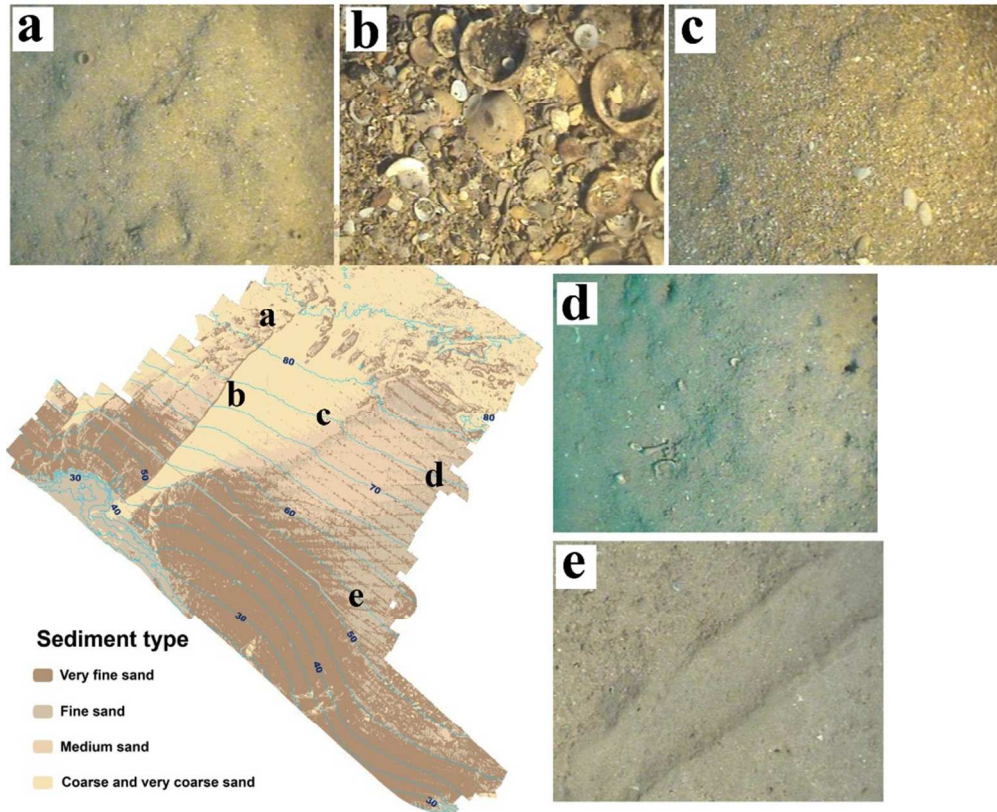


Figure 4. Sediment types distribution map obtained as a result of the supervised classification and underwater images of the surface of the seabed.
90x74mm (300 x 300 DPI)

Only

- 1 Table 1. Sedimentologic characteristics of the grab samples. VCS: very coarse sand;
 2 CS: coarse sands; MS: medium sand; FS: fine sand; and VFS: very fine sand.

Sediment type	N° of samples	Grain size (Phi)	Sorting	% gravel	% sand	% mud
VCS	4	-0,2±0,1	0,9±0,1	16,8±1,1	83,0±1,1	0,2±0,1
CS	9	0,3±0,3	0,8±0,1	7,6±2,7	92,1±2,8	0,4±0,4
MS	7	1,7±0,2	1,0±0,5	0,2±0,2	98,5±1,2	2,6±3,0
FS	28	2,6±0,3	0,8±0,3	0,9±1,1	92,1±4,8	7,0±4,7
VFS	10	3,3±0,3	0,8±0,1	0,9±0,6	79,2±12,7	19,9±12,0

3

For Review Only

1
2
3 1 Table 2. Number of samples, mean value and standard deviation for the variables and
4
5 2 sediment classes considered in the classification process. CS-VCS: coarse and very
6
7 3 coarse sand; MS: medium sand; FS: fine sand; and VFS: very fine sand.
8
9

Sediment class	N° of samples	Depth (m)	Backscatter (dB)	Slope (%)	Texture	Rugosity
CS-VCS	13	-63,44±13,62	-22,82±3,92	39,24±7,58	3,72±4,35	1,00±0,00
MS	7	-49,49±15,31	-29,83±3,39	35,64±6,56	2,96±1,29	1,00±0,00
FS	28	-43,11±14,63	-32,05±2,29	31,71±10,46	4,66±4,38	1,00±0,00
VFS	10	-56,60±12,38	-30,07±2,93	34,78±9,49	3,03±3,10	1,00±0,00

10
11
12
13
14
15
16 4
17
18
19
20
21
22
23
24
25
26
27
28
29
30
31
32
33
34
35
36
37
38
39
40
41
42
43
44
45
46
47
48
49
50
51
52
53
54
55
56
57
58
59
60

For Review Only

1 Table 3. Validation results obtained for classified data using unsupervised and
 2 supervised classification methods. Total classification accuracies: 30.77% and 76.92%,
 3 respectively. PA: Producer Accuracy; UA: User Accuracy.

Class name (Sediment type)	Reference	Unsupervised classification				Supervised classification			
		Classified	Correctly classified	PA (%)	UA (%)	Classified	Correctly classified	PA (%)	UA (%)
VCS-CS	3	1	0	0.0	0.0	1	1	33.3	100
MS	1	0	0	-	-	1	2	100	100
FS	5	5	3	60.0	60.0	8	5	100	62.5
VFS	3	6	1	33.3	14.3	2	2	66.7	100
Total	12	12	4			12	10		

4

- 1
2
3 1 Table 4. Results obtained for the Kappa statistic (k) for unsupervised and supervised
4
5 2 classifications.
6
7

Class name (Sediment type)	Unsupervised classification	Supervised classification
	Kappa	Kappa
VCS-CS	0.3	1.0
MS	0.0	1.0
FS	0.35	0.39
VFS	0.11	1.0
Total	0.19	0.66

3

For Review Only

- 1 Table 5. Number of pixels, % of assigned pixels and area assigned to each sediment
 2 type according to the unsupervised and supervised automatic classifications.

Class name (Sediment type)	Unsupevised classification			Supevised classification		
	N° of pixels	% of assigned pixles	Area (km ²)	N° of pixels	% of assigned pixles	Area (km ²)
VCS-CS	325579	25.3	8.1	362373	28.1	9.1
MS	205927	16.0	5.2	156890	12.2	3.9
FS	430859	33.5	10.8	513602	39.9	12.8
VFS	324907	25.2	8.1	254407	19.8	6.4
Total	1287272	100	32.2	1287272	100	32.2

3